Final version published as: Jones, M. R., Dyrager, C., Hoarau, M., Korshavn, K. J., Lim, M. H., Ramamoorthy, A., & Storr, T. (2016). Multifunctional quinoline-triazole derivatives as potential modulators of amyloid-β peptide aggregation. *Journal of Inorganic Biochemistry*, 158, 131-138. DOI: 10.1016/j.jinorgbio.2016.04.022

Multifunctional Quinoline-Triazole Derivatives as Potential Modulators of Aβ Peptide Aggregation

Michael R. Jones[a]†; Christine Dyrager[a], Marie Hoarau[a]; Kyle J. Korshavn[b]; Mi Hee Lim[c]; Ayyalusamy Ramamoorthy[bd]; Tim Storr[a];*

[a]*Department of Chemistry, Simon Fraser University, V5A-1S6, Burnaby, BC, Canada*

[b]*Department of Chemistry, University of Michigan, Ann Arbor, USA*

[c]*Department of Chemistry, Ulsan National Institute of Science and Technology (UNIST), Ulsan, Korea*

[d]*Department of Biophysics, University of Michigan, Ann Arbor, USA*

ABSTRACT: Metal ion dyshomeostasis is hypothesized to play a role in the toxicity and aggregation of the amyloid beta (Aβ) peptide, contributing to Alzheimer's disease (AD) pathology. We report on the synthesis and metal complexation ability of three bidentate quinoline-triazole derivatives 3-(4-(quinolin-2-yl)-1*H*-1,2,3-triazol-1-yl)propan-1-ol (**QOH)**, 4-(2-(4-(quinolin-2-yl)-1*H*-1,2,3-triazol-1-yl)ethyl)morpholine (**QMorph)**, and 4-(2-(4-(quinolin-2-yl)-1*H*-1,2,3-triazol-1-yl)ethyl)thiomorpholine (**QTMorph**). We further study the utility of these ligands to modulate Aβ peptide aggregation processes in the presence and absence of Cu^{2+} ions. Ligand-peptide interactions were first investigated using both 2-D ^{1}H-^{15}N SOFAST-HMQC NMR spectroscopy and molecular modeling techniques, indicating interactions with E3 and several residues in the hydrophobic region of Aβ. Native gel electrophoresis with western blotting along with transmission electron microscopy provided information on the ability of each ligand to modulate Aβ aggregation. While the ligands alone did not modify Aβ peptide aggregation at the 24 hour timepoint, signifying relatively weak ligand-peptide interactions, the ligands did modify the aggregation profile of the peptide in the presence of stoichiometric and suprastoichiometric Cu. Interestingly, the thioether derivative QTMorph exhibited the most pronounced effect on peptide aggregation in the presence of Cu. Overall, the quinoline-triazole ligand series were shown to interact with the hydrophobic region of the Aβ peptide, and modulate Cu-Aβ aggregation process.

1. Introduction

Alzheimer's disease (AD) is the most common form of dementia with an estimated 44 million cases worldwide.[1] Two pathological hallmarks are common to AD: insoluble amyloid-β (Aβ) aggregates, termed Aβ plaques, and neurofibrillary tangles that consist of hyperphosphorylated tau proteins.[2] The amyloid hypothesis has long been the dominant theory to explain the cause of AD, postulating that Aβ plaque depositions, or partially aggregated, soluble Aβ species, trigger a neurotoxic cascade causing AD pathology.[2a,2c,3] As a result, considerable research efforts have focused on the development of therapies, including anti-aggregation agents and Aβ antibodies, that regulate Aβ accumulation.[4]

Aggregation of the Aβ peptide is dependent on the conditions, and can follow a number of different pathways with specific aggregation intermediates.[5] However, these pathways eventually lead to the end-stage formation of insoluble amyloid plaques. Initiation of the Aβ aggregation process can occur via hydrophobic self-recognition interactions, specifically through peptide residues 17-21 (LVFFA),[6] resulting in the formation of oligomeric and fibrillar aggregates.[5] It has been proposed that oligomeric Aβ species, thought to be the most toxic form, also initially form via hydrophobic interactions between residues F19 and L34.[7] Thus, the development of small molecules capable of interfering with these interactions may inhibit the initial stages of Aβ aggregation, decreasing Aβ oligomer formation and associated neurotoxicity.[8] The interaction of metal ions with the Aβ peptide provides an additional pathway for aggregation, and *in vitro* studies have shown that the interaction of Aβ with metal ions (Cu, Fe, and Zn) can lead to the formation of soluble metalated forms, and/or insoluble Aβ aggregates.[9] Amyloid plaques isolated from human brain tissue contain abnormally high concentrations of Cu, Fe, and Zn ions in comparison to age-matched brain tissues,[10] implicating the role of these metal ions in AD plaque formation. Further *in vitro* studies have demonstrated that Cu and Fe ions potentiate the neurotoxicity of Aβ *via* redox-cycling and the production of reactive oxygen species in the presence of dioxygen.[11] There is extensive evidence of oxidative stress in AD, with early neuronal and pathological changes showing indications of oxidative damage.[12]

While the role of metal ions in the etiology of AD remains to be fully elucidated, targeting metallated Aβ species is a promising therapeutic strategy. Metal chelators can solubilize Aβ plaque deposits,[13] and, more impressively, show promise as AD therapeutics.[4a,14] Research efforts in this area have recently focused on the development of multifunctional molecules capable of binding metal ions, while also exhibiting additional beneficial properties such as Aβ aggregation inhibition, antioxidant activity, and/or acetylcholinesterase activity.[14a,14b,15]

In this report we detail the synthesis and characterization of a series of quinoline-triazole compounds (Figure 1) that incorporate a planar hydrophobic scaffold to enhance interactions with the Aβ peptide along with a metal-binding unit to modulate metal-Aβ interactions. Ligand-peptide interactions were investigated via 2-D NMR studies and

further information was gained from molecular docking simulations. The effect of these ligands on Aβ aggregation processes in the presence and absence of added Cu ions were explored by native gel electrophoresis and transmission electron microscopy (TEM) imaging. Our results show that the quinoline-triazole ligands weakly interact with the Aβ peptide in solution, and do not substantially alter the aggregation profile of the Aβ peptide under metal-free conditions. However, this ligand series does influence the Aβ peptide aggregation process in the presence of added Cu ions, which may play a role in modulating the formation of toxic metal-containing oligomeric species.

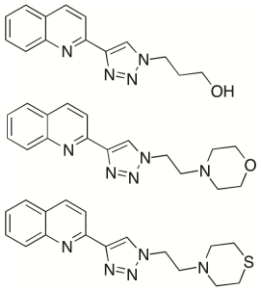

Figure 1. Chemical structures of **QOH** (top), **QMorph** (middle), and **QTMorph** (bottom).

2. Experimental

2.1. Materials and Methods. All reagents were purchased as reagent grade from commercial suppliers and used without further purification unless otherwise indicated. 2-Ethynylquinoline,[16] 2-azidoethyl-4-methylbenzenesulfonate,[17] 1-azidopropanol,[18] and 4-(2-azidoethyl)morpholine[15i] were synthesized according to previously reported literature protocols. ***Safety Precautions in Handling of Azides:*** Some azides are hazardous, and to avoid injury, follow safe laboratory practices, wear appropriate protective equipment and use appropriate shielding equipment. Azides can decompose violently upon heating, shock and/or friction. Only small quantities should be prepared at a single time. $A\beta_{1-42}$ peptide was purchased from 21st Century Biochemicals (Marlborough, MA, USA). $A\beta_{1-42}$ was dissolved in 2 ml hexafluoroisopropanol (HFIP) and sonicated for 5 minutes followed by incubation at 4°C overnight. The solution was then evaporated under a stream of N_2 and the film stored at -80°C.[19] ^{15}N-labeled $A\beta_{1-40}$ peptide was purchased from rPeptide. The gels were purchased from BioRad and membranes from PALL – Life Sciences. ^{1}H, ^{13}C, and 2-D ^{1}H-^{15}N SOFAST HMQC NMR spectra were recorded on a 600 MHz Bruker Avance NMR spectrometer. Mass spectra (positive ion) were obtained on an Agilent 6210 time-of-flight electrospray ionization mass spectrometer. High resolution electrospray ionization mass spectrometry (HR-ESI(+)-MS) was performed at the Mass Spectrometry and Proteomics Facility at the University of Notre Dame. Electronic spectra were obtained on a Cary 5000 spectrophotometer. FT-IR spectra were obtained using a Thermo Nicolet Nexus 670 FT-IR spectrophotometer equipped with a Pike MIRacle attenuated total reflection (ATR) sampling accessory.

2.2. Synthesis

2.2.1. Synthesis of 4-(2-azidoethyl)thiomorpholine

2-Azidoethyl-4-methylbenzenesulfonate[17] (2.004 g, 8.3 mmol), thiomorpholine (1.714 g, 16.6 mmol), and NEt_3 (3.362 g, 33.2 mmol) were dissolved in 10 ml MeCN in a 2-neck round bottom flask under N_2 atmosphere following a modified procedure.[15i] The solution was allowed to reflux for 4 days. The solution was concentrated *in vacuo*, dissolved in CH_2Cl_2 and washed with saturated $NaHCO_3$. The organic layers were combined, dried over $MgSO_4$, filtered, and concentrated *in vacuo*. The residue was purified by silica gel chromatography (90:10 CH_2Cl_2 / MeOH eluent) to afford 4-(2-azidoethyl)thiomorpholine as a dark yellow oil (0.891 g, 63 %). ^{1}H NMR ($CDCl_3$, 400 MHz): δ 3.31 (t, *J* = 5.9 Hz, 2H), 2.79 (t, *J* = 4.4 Hz, 4H), 2.70 (t, *J* = 5.6 Hz, 4H), 2.63 (t, *J* = 6.1 Hz, 2H). FT-IR (cm^{-1}): ν 2911 cm^{-1} (w, sh), 2811 cm^{-1} (w, sh), 2099 cm^{-1} (vs), 1284 cm^{-1} (w, sh).

*2.2.2. Synthesis of 3-(4-(quinolin-2-yl)-1H-1,2,3-triazol-1-yl)propan-1-ol (**QOH**)*

2-Ethynylquinoline[16] (0.037 g, 0.24 mmol) and 3-azido-1-propanol[18] (0.041 g, 0.40 mmol) were dissolved in 2 ml isopropanol. In 2 ml H_2O, $CuSO_4$ (0.003 g, 0.012 mmol) and *L*-ascorbic acid (0.021 g, 0.12 mmol) were dissolved and added to the isopropanol solution. The reaction was stirred at 298 K for 3 hours and then Chelex® resin was added in order to remove the Cu catalyst. The Chelex resin was filtered and the filtrate was concentrated *in vacuo*. The residue was purified by silica gel chromatography (90:10 CH_2Cl_2 / MeOH) to afford **QOH** as a brown solid (0.021 g, 34 % yield). ^{1}H NMR (CD_3OD, 400 MHz): δ 8.67 (s, 1H), 8.41 (d, *J* = 8.6 Hz, 1H), 8.21 (d, *J* = 8.6 Hz, 1H), 8.06 (d, *J* = 8.5 Hz, 1H), 7.94 (d, *J* = 8.2 Hz, 1H), 7.78 (t, *J* = 8.4 Hz, 1H), 7.60 (t, *J* = 8.1 Hz, 1H), 4.66 (t, *J* = 7.0 Hz, 2H), 3.65 (t, *J* = 6.1 Hz, 2H), 2.21 (quin, *J* = 6.1 Hz, 2H). ^{13}C NMR (CD_3OD, 100 MHz): δ 151.63, 149.26, 149.12, 138.95, 131.50, 129.56, 129.39, 129.25, 128.02, 125.35, 59.46, 48.72, 34.18. HR-ESI(+)-MS (*m/z*): $[M+H]^+$ Calcd for $[M+H]^+$ ($C_{14}H_{15}N_4O$), 255.1240; Found, 255.1274.

*2.2.3. Synthesis of 4-(2-(4-(quinolin-2-yl)-1H-1,2,3-triazol-1-yl)ethyl)morpholine (**QMorph**)*

2-Ethynylquinoline (0.049 g, 0.32 mmol) and 4-(2-azidoethyl)morpholine[15i] (0.059 g, 0.38 mmol) were dissolved in 2 ml isopropanol and the same procedure as detailed above for **QOH** was followed. The crude residue was purified by silica gel chromatography (90:10 CH_2Cl_2 / MeOH) to afford **QMorph** as a brown solid (0.059 g, 72% yield). ^{1}H NMR (CD_3OD, 400 MHz): δ 8.73 (s, 1H), 8.42 (d, *J* = 8.6 Hz, 1H), 8.23 (d, *J* = 8.6 Hz, 1H), 8.06 (d, *J* = 8.5 Hz, 1H), 8.14 (d, *J* = 8.5 Hz, 1H), 7.94 (d, *J* = 8.1 Hz, 1H), 7.77 (t, *J* = 7.1 Hz, 1H), 7.60 (t, *J* = 7.1 Hz, 1H), 4.68 (t, *J* = 6.2 Hz, 2H), 3.70 (t, *J* = 4.6 Hz, 4H), 2.94 (t, *J* = 6.3 Hz, 2H), 2.57 (t, *J* = 4.7 Hz, 4H). ^{13}C NMR ($CDCl_3$, 100 MHz): δ 151.67, 149.20, 148.94, 139.00, 131.53, 130.12, 129.47, 129.30, 126.45, 119.78, 67.98, 58.99, 54.69, 48.66 HR-ESI(+)-MS (*m/z*): $[M+H]^+$ Calcd for $[M+H]^+$ ($C_{17}H_{20}N_5O$), 310.1662; Found, 310.1682.

*2.2.4. Synthesis of 4-(2-(4-(quinolin-2-yl)-1H-1,2,3-triazol-1-yl)ethyl)thiomorpholine (**QTMorph**).*

2-Ethynylquinoline (0.111 g, 0.72 mmol) and 4-(2-azidoethyl)thiomorpholine (0.118 g, 0.65 mmol) were dissolved in 2 ml isopropanol and the same procedure as detailed above for **QOH** was followed. The residue was purified by silica gel chromatography (95:5 CH_2Cl_2 / MeOH eluent) to afford a brown solid (0.187 g, 89% yield). ^{1}H NMR ($CDCl_3$, 400 MHz): δ 8.42 (s, 1H), 8.33 (d, *J* = 8.5 Hz, 1H), 8.24 (d, *J* = 8.6 Hz, 1H), 8.07 (d, *J* = 8.6 Hz, 1H), 7.84 (d, *J* = 8.5 Hz, 1H), 7.73 (t, *J* = 8.5 Hz, 1H), 7.54 (t, *J* = 8.5 Hz, 1H), 4.53 (t, *J* = 6.0 Hz, 2H), 2.93 (t, *J* = 4.5 Hz, 4H), 2.81 (t, *J* = 6.1 Hz, 2H), 2.67 (t, *J* = 5.4 Hz, 4H). ^{13}C NMR ($CDCl_3$, 151 MHz): δ 150.63, 148.70, 148.16, 136.94, 129.81, 129.15, 127.88, 127.86, 126.42, 123.36, 118.78, 58.33, 55.09, 47.97, 28.05. HR-ESI(+)-MS (m/z): $[M+H]^+$ Calcd for $[M+H]^+$ ($C_{17}H_{20}N_5S$), 326.1434; Found, 326.1460.

2.3. Acidity Constant Determination

Acidity constants were measured by obtaining variable pH UV-vis and NMR spectra. Solutions of all three ligands (50 μM) were prepared in 0.1 M NaCl at pH 3 using HCl. Before obtaining UV-vis spectra, a pH electrode was calibrated using a 2-point method (pH 4.01 and pH 10.01 standard buffers). NaOH was used to increase the pH of the ligand solutions to obtain at least 30 spectra ranging from pH 3 – 12 from 600 – 190 nm. Spectral data was tabulated and analyzed using the HypSpec program (Protonic Software, UK).[20] A model was created for each ligand and simulated to fit the experimental data using selected wavelengths where significant spectral changes were observed. To complete the speciation diagrams variable pH ^{1}H NMR spectroscopy was also employed in order to probe regions of the molecule that do not undergo pK_a - dependent UV-vis changes. Solutions of 80 – 100 mg ligand in 8 mL of D_2O were prepared. NaOD and DCl were used to vary the pD of the solutions. Once the pH of the solution had stabilized, 500 μL of solution was placed in an NMR tube and ^{1}H NMR spectra obtained. Depending on the R-group, the pK_a values were determined by measuring the chemical shifts of the protons in the vicinity of the protonation site over a specific pH range. Data obtained was tabulated and analyzed using HypNMR (Protonic Software, UK).[20] The following equation (Eq. 1) was used to convert pD values to pH values.[21]

Eq. 1:

$$pK_a\,(H_2O) = (pK_a\,(D_2O) - 0.45)/1.015)$$

Speciation diagrams for **QOH**, **QMorph**, **QTMorph** were simulated using the HySS2009 program (Protonic Software, UK).[22]

2.4. Metal Stability Constant Measurements

Metal stability constant measurements were performed by obtaining ca. 30 UV-vis spectra of 75 μM ligand + 37.5 μM $CuCl_2$ in the pH range 3-11. HypSpec was used to analyze the data,[20] and a speciation model was developed and simulated to obtain the best fit to the experimental data.

2.5. Predictability of Drug-Like/BBB Permeability

Using the website molinspiration.com, several physicochemical properties were determined in order to predict the drug-like properties and blood-brain barrier (BBB) permeability of each ligand. cLogP, M_w, total potential surface area (TPSA), H-bond acceptors, and H-bond donors were calculated to determine the drug-like properties of each ligand.[23] Clark's equation[24] (Eq. 2) was used to determine the logBB, which is a reasonable indication of permeability through the blood-brain barrier:

Eq. 2:

$$logBB = -0.0148(TPSA) + 0.152(cLogP) + 0.139$$

2.6. 2-D SOFAST-HMQC NMR Spectroscopy

2-D band-**S**elective **O**ptimized **F**lip **A**ngle **S**hort **T**ransient (SOFAST) **H**eteronuclear **M**ultiple **Q**uantum **C**orrelation (HMQC) NMR experiments provide rapid, residue-specific insight into the protein environment. NMR samples were prepared from ^{15}N-labeled $A\beta_{1\text{-}40}$ (rPeptide) by first dissolving the peptide in 1% $NH_4OH_{(aq)}$ and lyophilizing to remove preformed aggregates. The peptide was re-dissolved in 3 μL of DMSO-d_6 and diluted into buffer for a final peptide concentration of 80 μM (pH 7.4, 20 mM PO_4, 50 mM NaCl, 7% D_2O v/v, 1% DMSO v/v). Spectra were taken at each titration point using a 600 MHz Bruker Avance NMR spectrometer equipped with a triple-resonance z-gradient cryogenic probe at 8 °C with 128 t_1 experiments, 128 scans, and a 100 ms recycle delay. The 2D ^{15}N-^{1}H SOFAST-HMQC data were processed using TOPSPIN 2.1 (Bruker) and resonance assignment was performed with Sparky 3.1134. Resonances were assigned based on previous assignments under similar conditions.[25] Chemical shift perturbation (CSP) was calculated using **Eq. 3**, where $\Delta\delta_H$ is defined as the change in ^{1}H chemical shift and $\Delta\delta_N$ is defined as the change in the ^{15}N chemical shift upon addition of ligand to the ^{15}N-labeled $A\beta_{1\text{-}40}$ relative to the chemical shifts of peptide in the absence of ligand.[26]

Eq. 3:

$$\Delta\delta_{NH} = \sqrt{\left(\Delta\delta_H{}^2\right) + \left(\frac{\Delta\delta_N}{5}\right)^2}$$

2.7. Molecular Modeling

Molecular docking studies were performed using Maestro from Schrödinger (Suite 2014).[27] The monomeric coordinates for the partially folded $A\beta_{1\text{-}40}$ peptide were obtained from the Protein Data Bank (PDB ID: 2LFM), enclosing an NMR-assembly of twenty conformers.[25a] The $A\beta_{1\text{-}40}$ structures and the ligands (**QOH**, **QMorph**, and **QTMorph**) were prepared and energy minimized according to standard procedures (Protein Preparation Wizard and LigPrep, respectively).[28] Subsequently, the Prime energy was calculated for the

processed peptide structures in order to confirm that there are no strains or clashes within the systems before the dockings were performed. Flexible dockings were performed with the twenty prepared conformers using the induced fit docking (IFD) protocol with extra precision (XP) settings for glide re-docking using the whole peptide structure as the grid centroid.[29] The docking results were evaluated and compared with the 2D SOFAST-HMQC data in order to find the lowest energy conformations that correlated with the chemical shift perturbation (CSP) data.

2.8. Native Gel Electrophoresis and Western Blotting

Aggregation of $A\beta_{1-42}$ in the presence of ligands and Cu was further evaluated by molecular weight separation on a 10 – 20% gradient tris-tricine gel (Bio-Rad #456-3114) and visualized using western blotting techniques. Each sample was incubated for 24 hours under constant agitation at 37 ^{o}C in a 96-well plate, covered with a lid and sealed with parafilm. Final concentrations, diluted in 0.1 M PBS pH 7.4, were as follows: 25 μM $A\beta_{1-42}$, 25 (1 eq.) and 35 μM (1.4 eq.) $CuCl_2$, 50 μM (2 eq.) and 125 μM (5 eq.) ligand. After 24 hours, samples were loaded onto the gel and run at 100 V for 100 minutes in a tricine running buffer, followed by transferring to a nitrocellulose membrane for 3 hours at 40 V in a 4 ^{o}C cold room. The membrane was blocked in 3 % BSA solution in tris-buffered saline containing 0.1 % Tween-20 (TBS-T) for 1 hour at room temperature, followed by incubation with a primary anti-Aβ antibody (6E10) overnight at room temperature under constant agitation. The membrane was washed 4 x 15 minutes with TBS buffer and then incubated at room temperature under constant agitation for 2 hours with a horseradish peroxidase conjugated goat anti-mouse secondary antibody in 2 % BSA solution. The membrane was washed with TBS buffer for 4 x 15 minutes, incubated with the Thermo Scientific Supersignal West Pico Chemiluminsecent Substrate kit (ThermoScientific #34087) for 5 minutes and visualized with a Fujifilm Luminescent imager.

2.9. Transmission Electron Microscopy (TEM)

Samples were prepared by following a previously reported procedure.[15h,15i] Briefly, 5 μL aliquots from the native gel electrophoresis experiments were placed onto a sheet of parafilm and incubated for 5 minutes on glow-discharged Formvar/Carbon 300-mesh grids (Electron Microscopy Sciences). Afterward, the grid was stained with syringe-filtered 5% uranyl acetate using 3 × 5 μL drops placed onto parafilm. The grid was placed on the first drop of uranyl acetate and immediately removed, repeated for the second drop, then placed on the third drop to incubate for 1 minute. Excess uranyl acetate was removed using a tissue between drops. Bright field images were obtained using a FEI Osiris operating at 200 kV and 9000X magnification.

3. Results

3.1. Ligand Design and Synthesis

A series of quinoline-triazole derivatives were synthesized in a modular fashion using Huisgen's 1,3-dipolar cycloaddition, a reaction that satisfies the criteria required for click chemistry (Figure 1).[30] A bidentate metal binding site was incorporated into the scaffold upon triazole formation, with variation of a peripheral R-group. The extended ring system of the quinoline-triazole derivatives was incorporated to enhance hydrophobic interactions between the ligands and the Aβ peptide in comparison to the previously reported pyridine-triazole series.[15i] Three quinoline-triazole derivatives were synthesized by reacting 2-ethynylquinoline with corresponding azides in the presence of a catalytic amount of $CuSO_4$ and *L*-ascorbic acid. This modular synthetic route allowed for the construction of three quinoline-triazoles in 34 – 89% yields.

3.2. Physicochemical Properties

Lipinski's rule of 5 describes parameters that predict whether a compound will exhibit favorable pharmacokinetic properties, which can inform potential BBB-permeability. These parameters include calculated partition coefficient (cLogP), molecular weight, and hydrogen bond acceptors and donors (HBA, HBD), and can be calculated using a web-based program.[31] These drug-like parameters can then be used to calculate a logBB value using Clark's equation (**Eq. 2**), providing a prediction of BBB-permeability.[24] LogBB values > 0.3 indicate a high probability of permeation through the BBB and values < -1.0 indicate low probability of BBB access.[24,32] The drug-like parameters and logBB values were determined for **QOH**, **QMorph**, **QTMorph** (Table S1). Based on Lipinski's rules, all three ligands passed the four criteria to determine drug-likeness including having a M_w < 500 g/mol, cLogP < 5, and H-bond donors and acceptors < 5 and < 10, respectively. In addition, the calculated TPSA values were within the criteria for BBB permeability. Using these parameters, LogBB values were calculated using Clark's equation (LogBB: **QOH** = -0.61; **QMorph** = -0.46; **QTMorph** = -0.24) which indicate that the quinoline-triazole ligands are predicted to have moderate BBB permeability.

3.3. Acidity Constant Measurements for QMorph, QOH, QTMorph

To determine the ligand species present at pH 7.4, variable pH UV-vis and ^{1}H NMR spectra were obtained for each ligand (Figures S1-S3) to determine the pK_a values of the ligand protonation sites. The quinoline-*N* pK_a value ranged from 3.43 – 3.66 (Table 1), which is lower in comparison to free quinoline (pK_a = 4.85).[33] Fitting the variable pH ^{1}H NMR data for **QMorph** and **QTMorph** provided similar pK_a values for the *N*-atom of the morpholine and thiomorpholine rings (Table 1). Interestingly, these values are lower in comparison to free morpholine and thiomorpholine (pK_a morpholine = 8.35, pK_a thiomorpholine = 8.48).[15i,34] It has been proposed that the distinct difference in morpholine and thiomorpholine pK_a values can be attributed to the steric and/or electronic effects of the triazole ring.[34b,35] The experimentally determined pK_a values show that each ligand will be neutral at physiological pH (pH 7.4).

Table 1. pK_a values and speciation at physiological pH as determined by variable pH UV-vis and NMR spectroscopy titrations.

	UV-vis	NMR	
	pK_a (Quinoline)	pK_a (R-group)	Speciation (pH 7.4)
QOH	3.66(3)	n/a	Neutral
QMorph	3.43(6)	5.1(1)	Neutral
QTMorph	3.43(3)	5.4(2)	Neutral

3.4. Metal Stability Constant Measurements.

Spectrophotometric titrations were employed to determine the Cu-binding affinity of each of the quinoline-triazole ligands. The pK_a values of each ligand were included in the fitting in order to obtain log *K* values. Solution speciation diagrams for each ligand with Cu^{2+} suggest that a mixture of 1:1 and 2:1 ligand:Cu^{2+} species exist at pH 7.4 (Figures 2, S4-5). Based on the stability constant measurements, the concentration of free Cu in solution at pH 7.4 was estimated as a pCu (pCu = -log[$Cu_{unchelated}$]) value (Table 2). The pCu value provides a direct estimate of metal-ligand affinity taking into account all relevant equilibria, and is dependent on ligand and metal concentration, temperature, ionic strength, and pH of the solution. [36] Our results show that the quinoline-triazole ligand series exhibit a moderate affinity for Cu^{2+} ($K_d \sim 10^{-6} - 10^{-5}$), at the lower end of the range required for competing with the Aβ peptide for Cu ions in solution.[15f]

3.5. Ligand- Aβ Peptide Interactions.

2-D ^{1}H-^{15}N SOFAST-HMQC NMR has been recently employed to evaluate ligand interactions with the Aβ peptide.[15d,37] These literature studies have used the less aggregation prone $A\beta_{1-40}$ isoform to limit aggregation during data collection and ensure all shifts are solely the result of peptide-ligand interactions and not peptide aggregation. In this report, ^{15}N-labeled $A\beta_{1-40}$ was incubated with 0-10 eq. of quinoline-triazole ligands and ligand interactions were quantified using the CSP (Equation 3). Further information was obtained via molecular docking studies by using an $A\beta_{1-40}$ structure in the absence of any additive (ie: SDS), which would be more biologically representative, to find low energy conformations that match the 2-D NMR CSP data. **QMorph** exhibited the largest CSP for amino acids valine-18 (V18) and phenylalanine-19 (F19), which are located in the hydrophobic region of Aβ (Figures 3 - 4). Interaction between **QMorph** and these amino acid residues may be attributed to hydrophobic interactions, including π – π stacking with the aromatic side chain of F19. Several weaker interactions were also observed including residues glutamic acid–3 (E3), and histidine–13 (H13) attributed to a combination of electrostatic interactions and H-bonding for the polar amino acids. A low energy molecular docking pose for **QMorph** with $A\beta_{1-40}$, that corresponds with the measured CSP from the 2D NMR experiments**,** shows a cis-*N*, *N* orientation of the quinolone and triazole rings with the morpholine moiety oriented towards the V18 and F19 side chains (Figure 4). In addition, the quinoline ring system is located within the van der Waals radius of the E3 backbone. These three residues exhibited the largest CSP values when interacting with QMorph (Figure 3).

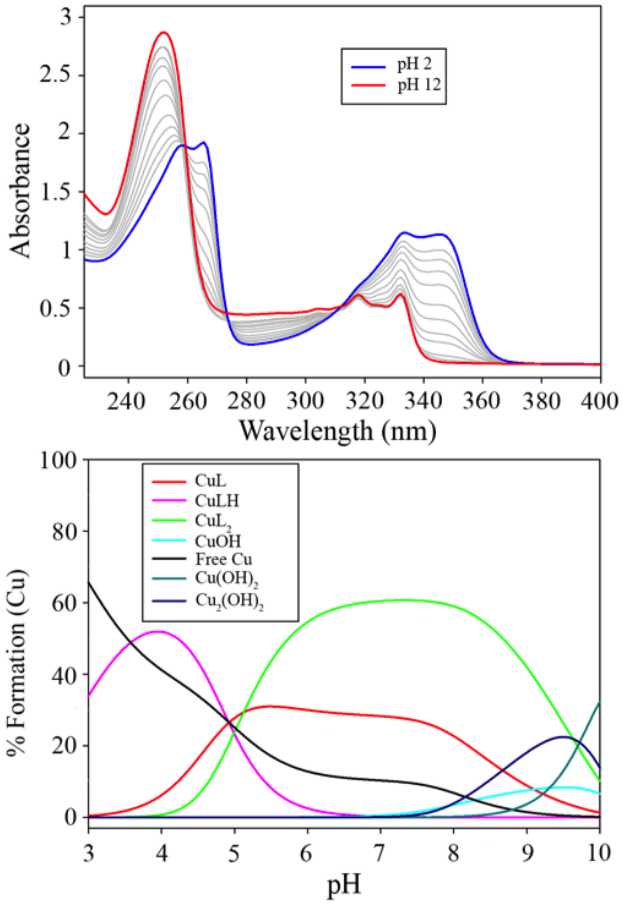

Figure 2. (Top) Variable pH UV-vis titration of 2:1 **QMorph**:Cu ranging from pH 2-12 in 0.1 M NaCl. (Bottom) Simulated species distribution plot using HypSpec and HySS.

Table 2. Stability constant measurements (log *K* and pCu) of each ligand with Cu^{2+}.

		log *K*		
	pCu (pH 7.4)	CuL	CuLH	CuL_2
QOH	4.9	4.31(3)	n/a	8.03(5))
QMorph	5.4	5.17(8)	10.10(1)	10.24(7)
QTMorph	4.9	4.34(1)	9.41(9)	8.48(5)

QTMorph exhibited large CSP with valine-18 (V18) and asparagine-27 (N27), but also with E3 in the hydrophilic region (Figure S6). Hydrophobic interactions between V18 and **QTMorph**, and hydrogen bonding or electrostatic interactions with E3 and N27, are most likely. A low energy molecular docking pose for **QTMorph** that best describes the 2D NMR interactions includes the quinoline ring positioned towards the V18 side chain, with the triazole ring within the van der Waals radius of the E3 side chain (Figure S7). E3 and

V18 were found to have the largest CSP values during the 2D NMR experiment.

In comparison to **QMorph** and **QTMorph**, both of which exhibited large CSP with a small number of amino acid residues, **QOH** showed significant interactions with a greater number of amino acids across the $A\beta_{1-40}$ peptide (Figure S8). For example, **QOH** caused the most dramatic CSP in residues E3, H13, L17, F20, aspartic acid–23 (D23), and methionine –35 (M35). The pose that best describes the **QOH**-$A\beta_{1-40}$ interaction involves the quinoline ring situated within the van der Waals radius of both H13 and F20 side chains with the benzene ring oriented towards the imidazole of H13 and the pyridine ring towards the phenyl side chain of F20 (Figure S9). The propanol side chain of **QOH** is within the van der Waals radius of the D23 side chain.

Interestingly, the interaction with the E3 residue is common across all three quinoline derivatives, potentially due to the flexible N-terminus of Aβ peptide. Aggregation of the Aβ peptide is hypothesized to initiate via interactions in the hydrophobic region of the peptide, specifically ^{17}LVFFA^{21}.[38] The quinoline-triazole ligands exhibited several significant interactions within the ^{17}LVFFA^{21} region, and thus may be able to inhibit Aβ aggregation processes at an early stage.

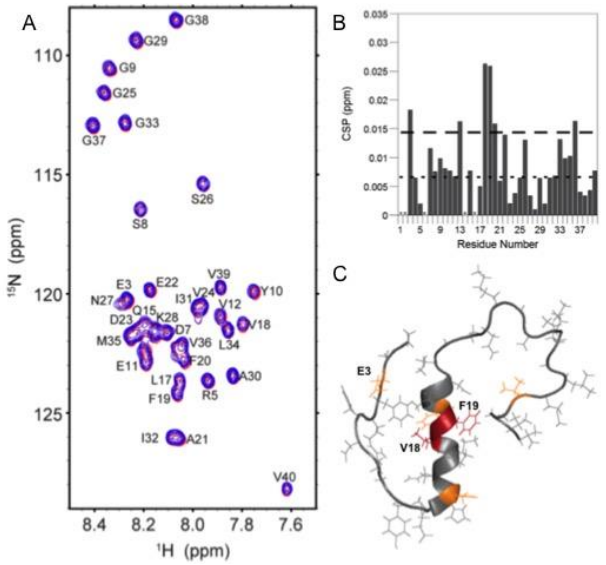

Figure 3. (A) 2D SOFAST-HMQC NMR spectra of 80 μM $A\beta_{1-40}$ and 0-10 eq. **QMorph** (Red = 0 eq. **QMorph**, Blue = 10 eq. **QMorph**). (B) Chemical shift changes in relation to specific $A\beta_{1-40}$ residues. The dotted line represents the average CSP for the entire experiment and the long dashed line represents one standard deviation above the average CSP. Residues denoted with * indicates the inability to resolve that specific residue. (C) Solution NMR structure of $A\beta_{1-40}$ (PDB 2LFM)[25a] with residues exhibiting a CSP > 0.02ppm highlighted in red and residues with a CSP between 0.01 – 0.02 highlighted in yellow.

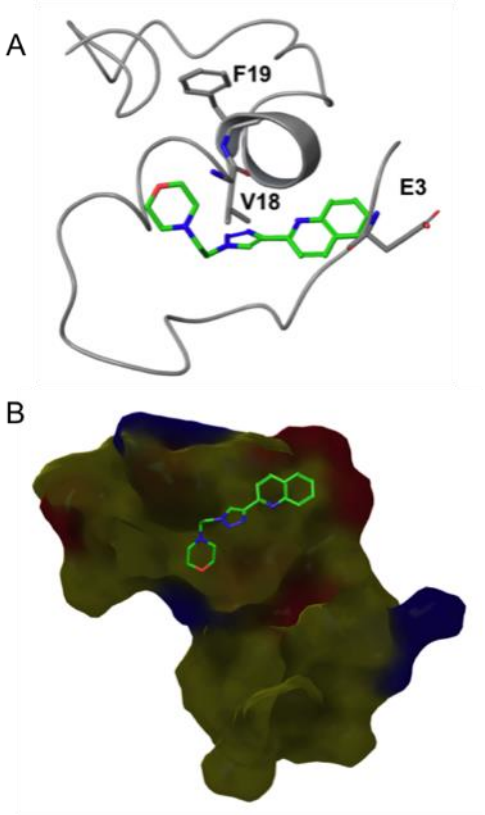

Figure 4. Molecular docking pose of QMorph with $A\beta_{1-40}$ (PDB: 2LFM). (A) Amino acid interactions with the peptide include V18, F19, and E3 side chains. (B) **QMorph** has a favourable pose that resides in a hydrophobic region on $A\beta_{1-40}$. (Peptide surface representation showing residue charge: Red = negatively charged; Blue = positively charged; Yellow/Green = neutral).

3.6. Aβ-Aggregation Experiments.

Native gel electrophoresis/Western blotting, and transmission electron microscopy (TEM), were used to examine the effect of the quinoline-triazole ligands on $A\beta_{1-42}$ aggregation in the absence and presence of added Cu ions. The longer $A\beta_{1-42}$ variant was used in these studies as it is more prone to aggregation and neurotoxicity.[39] We first evaluated the ability of the quinoline-triazole ligands to interfere with Aβ peptide aggregation in the absence of added Cu. This provided information on the ability of the ligands to interfere with peptide aggregation via disruption of hydrophobic peptide-peptide interactions. Interestingly, no changes in the Aβ aggregation profile were observed in the presence of the ligands at the two different concentrations studied (2 and 5 eq.; Figure S10). These results suggest that the ligand-peptide interactions observed by 2-D NMR, and further investigated by molecular docking studies, are likely too weak to influence the $A\beta_{1-42}$ aggregation pathway after 24 hours. It is however possible that the ligands do influence peptide aggregation at earlier timepoints.

We then evaluated the ability of the ligands to influence peptide aggregation in the presence of stoichiometric and excess amounts of Cu^{2+}. Studies have also shown that the Aβ

peptide is able to bind *ca*. 1.4 - 2 eq. Cu^{2+} in the presence of excess Cu^{2+} while in the absence of ligands, suggesting that a second, lower-affinity Cu^{2+} binding site exists on the Aβ peptide.[40 41]

When $A\beta_{1\text{-}42}$ was incubated in the absence of Cu^{2+} or ligands, significant amounts of high M_w species are observed along with a small amount of low M_w species in the 10 – 25 kDa region (Figure 5, lane 1). TEM measurements show the expected formation of fibrillar networks (Figure S11A).[42] Incubation of $A\beta_{1\text{-}42}$ in the presence of 1 eq. $CuCl_2$, results in the formation of low M_w oligomeric species, in line with previous reports (Figure 5, lane 2).[9c,40b] In the presence of excess Cu ions (1.4 eq.), a range of M_w were observed after incubation, including both low M_w oligomeric species (10 – 25 kDa range) and high M_w aggregates (100 – 250 kDa range) (Figure 5, lane 3).[9d,42a,43] Incubation of $A\beta_{1\text{-}42}$ with Cu (1:1 and 1.4:1) results in the formation of amorphous aggregates, and absence of fibrillar structures as observed in the TEM measurements (Figures S11B and S11C). Upon incubation of 5 eq. **QOH**/**QMorph**/**QTMorph** with 1 eq. $CuCl_2$ in the presence of $A\beta_{1\text{-}42}$, a small increase in high M_w species is observed when compared to lane 2 containing no ligands (Figure 5, lanes 4-6). No other substantial changes are observed on the gel, and TEM analysis shows that the Cu-Aβ aggregates are unchanged in the absence or presence of the quinoline-triazole ligands (Figure S11D-F). In combination, these results suggest that Cu-Aβ interactions (1:1 concentration ratio) and associated aggregation has not been perturbed significantly in the presence of the quinoline triazole ligands at the 24 hour timepoint.

Comparison of lanes 3 (1.4:1 Cu:$A\beta_{1\text{-}42}$) and 7 (5 eq. **QOH**) in Figure 5 shows a significant decrease in high M_w species and little change in the amount of low M_w species in the 10 – 25 kDa range with added ligand. A similar aggregation profile is observed for **QMorph** under the same conditions (Figure 5, lane 8). TEM analysis shows the presence of amorphous aggregates under these conditions (Figure S11H), with a pattern similar to the 1:1 Cu:$A\beta_{1\text{-}42}$ experiments. The results suggest that the **QOH** and **QMorph** ligands are able to modulate $A\beta_{1\text{-}42}$ aggregation in the presence of excess Cu ions. Interestingly, when 5 eq. **QTMorph** was incubated in the presence of 1.4 eq. $CuCl_2$ and 1 eq. $A\beta_{1\text{-}42}$, a large range of M_w species was detected (Figure 5, lane 9). This suggests that either **QTMorph**, a Cu-**QTMorph** complex, or a combination of both is reacting with the $A\beta_{1\text{-}42}$ peptide causing the formation of a wide range of Aβ species. Interestingly, such reactivity is not observed at lower Cu^{2+} concentrations in the presence of 5 eq. **QTMorph** (Figure 5, lane 6 vs. lane 9).

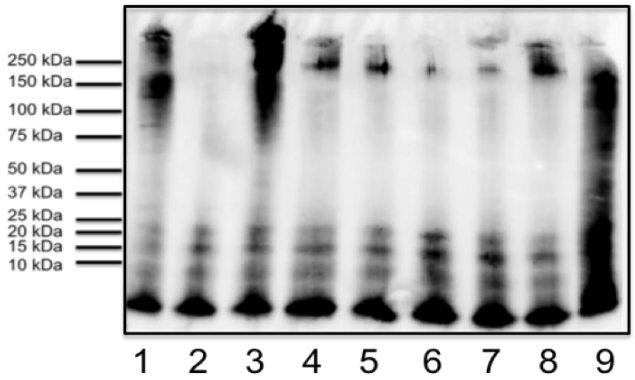

Figure 5. Native gel electrophoresis of $A\beta_{1\text{-}42}$ in the absence and presence of 1 eq. or 1.4 eq. Cu^{2+} and 5 eq. quinoline-triazole derivatives. Conditions: 25 μM $A\beta_{1\text{-}42}$, 25 (1 eq.) and 35 (1.4 eq.) μM Cu^{2+}, 5 eq. ligand, PBS pH 7.4, 24 hour incubation at 37 °C. Lanes: 1 - $A\beta_{1\text{-}42}$ only; 2 - $A\beta_{1\text{-}42}$ + 1 eq. Cu^{2+}; 3 - $A\beta_{1\text{-}42}$ + 1.4 eq. Cu^{2+}; 4 - $A\beta_{1\text{-}42}$ + 1 eq. Cu^{2+} + 5 eq. **QOH**; 5 - $A\beta_{1\text{-}42}$ + 1 eq. Cu^{2+} + 5 eq. **QMorph**; 6 - $A\beta_{1\text{-}42}$ + 1 eq. Cu^{2+} + 5 eq. **QTMorph**; 7 - $A\beta_{1\text{-}42}$ + 1.4 eq. Cu^{2+} + 5 eq. **QOH**; 8 - $A\beta_{1\text{-}42}$ + 1.4 eq. Cu^{2+} + 5 eq. **QMorph**; 9 - $A\beta_{1\text{-}42}$ + 1.4 eq. Cu^{2+} + 5 eq. **QTMorph**.

4. Summary

A series of three bidentate quinoline-triazole ligands were investigated for their ability to interact with the Aβ peptide in solution, and modulate Aβ aggregation in the presence and absence of added Cu ions. 2-D ^{1}H – ^{15}N SOFAST NMR studies showed that **QMorph** and **QTMorph** interacted with specific amino acid residues in the hydrophobic region (^{17}LVFFA^{21}), along with the E3 residue in the hydrophilic region, while **QOH** demonstrated relatively non-specific amino acid interactions over the length of the peptide. Native gel electrophoresis demonstrated that the ligands did not alter Aβ peptide aggregation in the absence of Cu after 24 hours, showing that the ligand-peptide interactions are likely not strong enough to significantly alter the aggregation process under the experimental conditions. When the ligands were incubated in the presence of a 1:1 mixture of Cu^{2+} + $A\beta_{1\text{-}42}$, oligomeric species were primarily observed with only minor changes in the peptide aggregation pattern in comparison to the control (1:1 Cu: $A\beta_{1\text{-}42}$). More significant changes in the aggregation pattern were observed with an increased ratio of Cu^{2+} to $A\beta_{1\text{-}42}$ (1.4:1), showing that the quinoline-triazole ligands are capable of modulating $A\beta_{1\text{-}42}$ aggregation in the presence of excess Cu ions.

A range of Cu-Aβ dissociation constants have been reported (ca. $K_d \sim 10^{-11} – 10^{-7}$)[15g,39a] and it is expected that ligands with a K_d value within this range will be needed to mediate Cu-Aβ aggregation processes.[15f] The measured K_d values for the quinoline-triazole series are just outside of this range ($K_d = 10^{-6} – 10^{-5}$) resulting in limited changes to the aggregation profile for 1:1 Cu^{2+}-Aβ in the presence of these ligands. Indeed, ligand K_d values of $> 10^{-5}$ lead to limited reactivity against Cu^{2+} + Aβ.[44] It has been reported that the Aβ peptide has a second lower affinity binding site for Cu^{2+}, with

an approximate K_d of 10^{-5}.[41] The quinoline-triazole series modulated Cu-Aβ aggregation processes in the presence of excess Cu ions (1.4:1), as the ligand K_d values are a likely better match with this lower affinity Cu-binding site. We have now focused on the design of ligands with enhanced peptide interactions, and a higher affinity for Cu.

Supporting Information

This material is available free of charge via the Internet at http://pubs.acs.org.

> Additional details describing Lipinski's drug-like properties for each ligand, solution speciation diagrams for each ligand and ligand + Cu experiments, 2-D NMR spectra, molecular modeling images, and transmission electron microscopy images can be found here.

Author Information

Corresponding Author

*E-mail: tim_storr@sfu.ca

Present Addresses

† Cumming School of Medicine, Hotchkiss Brain Institute Department of Clinical Neurosciences, University of Calgary, 3330 Hospital Drive, NW, Calgary, AB, Canada, T2N 4N1.

Notes

The authors declare no competing financial interest.

Acknowledgements

This work was supported by an NSERC Discovery Grant and a Michael Smith Career Investigator Award (to T.S.); Alzheimer Society of Canada for a doctoral award (to M.R.J.), an International postdoctoral grant from the Swedish Research Council (Dnr: 350-2012-239 to C.D.). Additional support is acknowledged from the Protein Folding Initiative at the University of Michigan (A. R. and M. H. L.) and the National Research Foundation of Korea (NRF) grant funded by the Korean government [NRF-2014S1A2A2028270] (to M. H. L. and A. R.)

References

1. Prince, M. W., A.; Guerchet, M.; Ali, G-C.; Wu, Y-T.; Prina, M. World Alzheimer Report 2015. [Online Early Access]. Published Online: 2015.

2. (a) Hardy, J.; Selkoe, D. J. *Science* **2002**, *297*, 353. (b) Selkoe, D. J. *Alzheimer's Disease: Genes, Proteins, and Therapy*, 2001; Vol. 81. (c) Selkoe, D. J. *Nat. Med.* **2011**, *17*, 1693. (d) Selkoe, D. J. *Neuron* **1991**, *6*, 487. (e) Selkoe, D. J.; Schenk, D. *Annu. Rev. Pharmacol. Toxicol.* **2003**, *43*, 545.

3. Abbott, A. *Nature* **2008**, *456*, 161.

4. (a) Chiang, L.; Jones, M. R.; Ferreira, C. L.; Storr, T. *Curr. Top. Med. Chem.* **2012**, *12*, 122. (b) Wang, Q.; Yu, X.; Li, L.; Zheng, J. *Curr. Pharm. Des.* **2014**, *20*, 1223. (c) DeToma, A. S.; Salamekh, S.; Ramamoorthy, A.; Lim, M. H. *Chem. Soc. Rev.* **2012**, *41*, 608. (d) Goure, W. F.; Krafft, G. A.; Jerecic, J.; Hefti, F. *Alz. Res. Ther.* **2014**, *6*, 42. (e) Wang, Y. J. *Nat. Rev. Neurol.* **2014**, *10*, 188.

5. Hane, F.; Leonenko, Z. *Biomolecules* **2014**, *4*, 101.

6. (a) Pithadia, A. S.; Lim, M. H. *Curr. Opin. Chem. Biol.* **2012**, *16*, 67. (b) Tjernberg, L. O.; Lilliehöök, C.; Callaway, D. J. E.; Näslund, J.; Hahne, S.; Thyberg, J.; Terenius, L.; Nordstedt, C. *J. Biol. Chem.* **1997**, *272*, 12601. (c) Tjernberg, L. O.; Näslund, J.; Lindqvist, F.; Johansson, J.; Karlström, A. R.; Thyberg, J.; Terenius, L.; Nordstedt, C. *J. Biol. Chem.* **1996**, *271*, 8545.

7. (a) Haass, C.; Selkoe, D. J. *Nat. Rev. Mol. Cell Biol.* **2007**, *8*, 101. (b) Walsh, D. M.; Selkoe, D. J. *J. Neurochem.* **2007**, *101*, 1172.

8. Das, A. K.; Rawat, A.; Bhowmik, D.; Pandit, R.; Huster, D.; Maiti, S. *ACS Chem. Neurosci.* **2015**, *6*, 1290.

9. (a) Bush, A. I.; Pettingell, W. H.; Multhaup, G.; Paradis, M. d.; Vonsattel, J.-P.; Gusella, J. F.; Beyreuther, K.; Masters, C. L.; Tanzi, R. E. *Science* **1994**, *265*, 1464. (b) Smith, D. P.; Ciccotosto, G. D.; Tew, D. J.; Fodero-Tavoletti, M. T.; Johanssen, T.; Masters, C. L.; Barnham, K. J.; Cappai, R. *Biochemistry* **2007**, *46*, 2881. (c) Sharma, A. K.; Pavlova, S. T.; Kim, J.; Kim, J.; Mirica, L. M. *Metallomics* **2013**, *5*, 1529. (d) House, E.; Collingwood, J.; Khan, A.; Korchazkina, O.; Berthon, G.; Exley, C. *J Alzheimers Dis* **2004**, *6*, 291.

10. (a) Lovell, M. A.; Robertson, J. D.; Teesdale, W. J.; Campbell, J. L.; Markesbery, W. R. *J. Neurol. Sci.* **1998**, *158*, 47. (b) Miller, L. M.; Wang, Q.; Telivala, T. P.; Smith, R. J.; Lanzirotti, A.; Miklossy, J. *J. Struct. Biol.* **2006**, *155*, 30. (c) Squitti, R. *Frontiers in Bioscience-Landmark* **2012**, *17*, 451.

11. (a) Huang, X.; Atwood, C. S.; Hartshorn, M. A.; Multhaup, G.; Goldstein, L. E.; Scarpa, R. C.; Cuajungco, M. P.; Gray, D. N.; Lim, J.; Moir, R. D.; Tanzi, R. E.; Bush, A. I. *Biochemistry* **1999**, *38*, 7609. (b) Huang, X.; Cuajungco, M. P.; Atwood, C. S.; Hartshorn, M. A.; Tyndall, J. D. A.; Hanson, G. R.; Stokes, K. C.; Leopold, M.; Multhaup, G.; Goldstein, L. E.; Scarpa, R. C.; Saunders, A. J.; Lim, J.; Moir, R. D.; Glahe, C.; Bowden, E. F.; Masters, C. L.; Fairlie, D. P.; Tanzi, R. E.; Bush, A. I. *J. Biol. Chem.* **1999**, *274*, 37111.

12. (a) Nunomura, A.; Perry, G.; Aliev, G.; Hirai, K.; Takeda, A.; Balraj, E. K.; Jones, P. K.; Ghanbari, H.; Wataya, T.; Shimohama, S.; Chiba, S.; Atwood, C. S.; Petersen, R. B.; Smith, M. A. *J. Neuropathol. Exp. Neurol.* **2001**, *60*, 759. (b) Cho, D. H.; Nakamura, T.; Fang, J. G.; Cieplak, P.; Godzik, A.; Gu, Z.; Lipton, S. A. *Science* **2009**, *324*, 102.

13. Cherny, R. A.; Legg, J. T.; McLean, C. A.; Fairlie, D. P.; Huang, X.; Atwood, C. S.; Beyreuther, K.; Tanzi, R. E.; Masters, C. L.; Bush, A. I. *J. Biol. Chem.* **1999**, *274*, 23223.

14. (a) Telpoukhovskaia, M. A.; Orvig, C. *Chem. Soc. Rev.* **2013**, *42*, 1836. (b) Rodríguez-Rodríguez, C.; Telpoukhovskaia, M.; Orvig, C. *Coord. Chem. Rev.* **2012**, *256*, 2308. (c) Beck, M. W.; Pithadia, A. S.; DeToma, A. S.; Korshavn, K. J.; Lim, M. H. In *Ligand Design in Medicinal Inorganic Chemistry*; John Wiley & Sons, Ltd: 2014, p 257. (d) Crapper McLachlan, D. R.; Dalton, A. J.; Kruck, T. P.; Bell, M. Y.; Smith, W. L.; Kalow, W.; Andrews, D. F. *Lancet* **1991**, *337*, 1304. (e) Ritchie, C. W.; Bush, A. I.; Mackinnon, A.; Macfarlane, S.; Mastwyk, M.; MacGregor, L.; Kiers, L.; Cherny, R.; Li, Q.-X.; Tammer, A.; Carrington, D.; Mavros, C.; Volitakis, I.; Xilinas, M.; Ames, D.; Davis, S.; Beyreuther, K.; Tanzi, R. E.; Masters, C. L. *Arch. Neurol.* **2003**, *60*, 1685. (f) Lannfelt, L.; Blennow, K.; Zetterberg, H.; Batsman, S.; Ames, D.; Hrrison, J.; Masters, C. L.; Targum, S.; Bush, A. I.; Murdoch, R.; Wilson, J.; Ritchie, C. W.; Grp, P. E. S. *Lancet Neurol.* **2008**, *7*, 779. (g) Crouch, P. J.; Savva, M. S.; Hung, L. W.; Donnelly, P. S.; Mot, A. I.; Parker, S. J.; Greenough, M. A.; Volitakis, I.; Adlard, P. A.; Cherny, R. A.; Masters, C. L.; Bush, A. I.; Barnham, K. J.; White, A. R. *J. Neurochem.* **2011**, *119*, 220. (h) Kenche, V. B.; Barnham, K. J. *Br. J. Pharmacol.* **2011**, *163*, 211. (i) Galimberti, D.; Scarpini, E. *J. Neurol.* **2012**, *259*, 201. (j) Derrick, J. S.; Lim, M. H. *ChemBioChem* **2015**, *16*, 887.

15. (a) Geldenhuys, W. J.; Van der Schyf, C. J. *Exp. Opin. Drug. Disc.* **2013**, *8*, 115. (b) Bajda, M.; Guzior, N.; Ignasik, M.; Malawska, B. *Curr. Med. Chem.* **2011**, *18*, 4949. (c) Bolognesi, M. L.; Melchiorre, C.; Van der Schyf, C. J.; Youdim, M. In *Designing Multi-Target Drugs*; The Royal Society of Chemistry: 2012, p 290. (d) Gonzalez, P.; da Costa, V. C.; Hyde, K.; Wu, Q.; Annunziata, O.; Rizo, J.; Akkaraju, G.; Green, K. N. *Metallomics* **2014**, *6*, 2072. (e) Scott, L. E.; Orvig, C. *Chem. Rev.* **2009**. (f) Savelieff, M. G.; DeToma, A. S.; Derrick, J. S.; Lim, M. H. *Acc. Chem. Res.* **2014**, *47*, 2475. (g) Savelieff, M. G.; Lee, S.; Liu, Y.; Lim, M. H. *ACS Chem. Biol.* **2013**, *8*, 856. (h) Gomes, L. M. F.; Vieira, R. P.; Jones, M. R.; Wang, M. C. P.; Dyrager, C.; Souza-Fagundes, E. M.; Da Silva, J. G.; Storr, T.; Beraldo, H. *J. Inorg. Biochem.* **2014**, *139*, 106. (i) Jones, M. R.; Service, E. L.; Thompson, J. R.; Wang, M. C. P.; Kimsey, I. J.;

DeToma, A. S.; Ramamoorthy, A.; Lim, M. H.; Storr, T. *Metallomics* **2012**, *4*, 910. (j) Derrick, J. S.; Kerr, R. A.; Nam, Y.; Oh, S. B.; Lee, H. J.; Earnest, K. G.; Suh, N.; Peck, K. L.; Ozbil, M.; Korshavn, K. J.; Ramamoorthy, A.; Prabhakar, R.; Merino, E. J.; Shearer, J.; Lee, J.-Y.; Ruotolo, B. T.; Lim, M. H. *J. Am. Chem. Soc.* **2015**, *137*, 14785.
16. Rodríguez, J. G.; de los Rios, C.; Lafuente, A. *Tetrahedron* **2005**, *61*, 9042.
17. Demko, Z. P.; Sharpless, K. B. *Org. Lett.* **2001**, *3*, 4091.
18. Hong, V.; Presolski, S. I.; Ma, C.; Finn, M. G. *Angew. Chem. Int. Ed.* **2009**, *48*, 9879.
19. Stine, W. B.; Jungbauer, L.; Yu, C.; LaDu, M. J. *Methods in molecular biology (Clifton, N.J.)* **2011**, *670*, 13.
20. Gans, P. S., A.; Vacca, A. *Ann. Chim.* **1999**, *89*, 45.
21. Song, B.; Kurokawa, G. S.; Liu, S.; Orvig, C. *Canadian Journal of Chemistry-Revue Canadienne De Chimie* **2001**, *79*, 1058.
22. Alderighi, L.; Gans, P.; Ienco, A.; Peters, D.; Sabatini, A.; Vacca, A. *Coord. Chem. Rev.* **1999**, *184*, 311.
23. Leeson, P. *Nature* **2012**, *481*, 455.
24. Clark, D. E.; Pickett, S. D. *Drug Discov. Today* **2000**, *5*, 49.
25. (a) Vivekanandan, S.; Brender, J. R.; Lee, S. Y.; Ramamoorthy, A. *Biochem. Biophys. Res. Commun.* **2011**, *411*, 312. (b) Yoo, S. I.; Yang, M.; Brender, J. R.; Subramanian, V.; Sun, K.; Joo, N. E.; Jeong, S. H.; Ramamoorthy, A.; Kotov, N. A. *Angew. Chem. Int. Ed.* **2011**, *50*, 5110. (c) Fawzi, N. L.; Ying, J.; Torchia, D. A.; Clore, G. M. *J. Am. Chem. Soc.* **2010**, *132*, 9948.
26. Williamson, M. P. *Progress in Nuclear Magnetic Resonance Spectroscopy* **2013**, *73*, 1.
27. Maestro, v., Schrodinger, LLC, New York, NY, 2014.
28. (a) Sastry, G. M.; Adzhigirey, M.; Day, T.; Annabhimoju, R.; Sherman, W. *J. Comput. Aided Mol. Des.* **2013**, *27*, 221. (b) Shelley, J.; Cholleti, A.; Frye, L.; Greenwood, J.; Timlin, M.; Uchimaya, M. *J. Comput. Aided Mol. Des.* **2007**, *21*, 681.
29. (a) Sherman, W.; Beard, H. S.; Farid, R. *Chem. Biol. Drug Des.* **2006**, *67*, 83. (b) Friesner, R. A.; Banks, J. L.; Murphy, R. B.; Halgren, T. A.; Klicic, J. J.; Mainz, D. T.; Repasky, M. P.; Knoll, E. H.; Shelley, M.; Perry, J. K.; Shaw, D. E.; Francis, P.; Shenkin, P. S. *J. Med. Chem.* **2004**, *47*, 1739. (c) Halgren, T. A.; Murphy, R. B.; Friesner, R. A.; Beard, H. S.; Frye, L. L.; Pollard, W. T.; Banks, J. L. *J. Med. Chem.* **2004**, *47*, 1750.
30. (a) Rostovtsev, V. V.; Green, L. G.; Fokin, V. V.; Sharpless, K. B. *Angew. Chem. Int. Ed.* **2002**, *41*, 2596. (b) Tornoe, C. W.; Christensen, C.; Meldal, M. *J. Org. Chem.* **2002**, *67*, 3057.
31. molinspiration.com.
32. Abraham, M. H.; Takács-Novák, K.; Mitchell, R. C. *J. Pharm. Sci.* **1997**, *86*, 310.
33. Braude, E. A. N., F. C. *Determination of Organic Structures by Physical Methods*; Academic Press: New York, New York, 1955; Vol. 1.
34. (a) Hall, H. K. *J. Am. Chem. Soc.* **1957**, *79*, 5441. (b) Cook, A. G.; Wesner, L. R.; Folk, S. L. *J. Org. Chem.* **1997**, *62*, 7205. (c) Martin, R. E.; Plancq, B.; Gavelle, O.; Wagner, B.; Fischer, H.; Bendels, S.; Müller, K. *ChemMedChem* **2007**, *2*, 285. (d) Coello, A.; Meijide, F.; Tato, J. V. *J. Chem. Soc. Perkin Trans. 2* **1989**, 1677.
35. Hall, H. K.; Bates, R. B. *Tetrahedron Lett.* **2012**, *53*, 1830.
36. (a) Fahrni, C. J.; O'Halloran, T. V. *J. Am. Chem. Soc.* **1999**, *121*, 11448. (b) Martell, A. E.; Hancock, R. D. *Metal Complexes in Aqueous Solutions*; Springer US, 1996. (c) Chiu, Y.-H.; Canary, J. W. *Inorg. Chem.* **2003**, *42*, 5107.
37. (a) Lee, S.; Zheng, X. Y.; Krishnamoorthy, J.; Savelieff, M. G.; Park, H. M.; Brender, J. R.; Kim, J. H.; Derrick, J. S.; Kochi, A.; Lee, H. J.; Kim, C.; Ramamoorthy, A.; Bowers, M. T.; Lim, M. H. *J. Am. Chem. Soc.* **2014**, *136*, 299. (b) DeToma, A. S.; Krishnamoorthy, J.; Nam, Y.; Lee, H. J.; Brender, J. R.; Kochi, A.; Lee, D.; Onnis, V.; Congiu, C.; Manfredini, S.; Vertuani, S.; Balboni, G.; Ramamoorthy, A.; Lim, M. H. *Chem. Sci.* **2014**, *5*, 4851.
38. (a) Pithadia, A. S.; Lim, M. H. *Curr. Opin. Chem. Biol.* **2012**, *16*, 67. (b) Kim, W.; Hecht, M. H. *Proc. Nat. Acad. Sci.* **2006**, *103*, 15824.
39. (a) Kepp, K. P. *Chem. Rev.* **2012**, *112*, 5193. (b) Jakob-Roetne, R.; Jacobsen, H. *Angew. Chem. Int. Ed.* **2009**, *48*, 3030.
40. (a) Pedersen, J. T.; Østergaard, J.; Rozlosnik, N.; Gammelgaard, B.; Heegaard, N. H. H. *J. Biol. Chem.* **2011**, *286*, 26952. (b) Pedersen, J. T.; Teilum, K.; Heegaard, N. H. H.; Østergaard, J.; Adolph, H.-W.; Hemmingsen, L. *Angew. Chem. Int. Ed.* **2011**, *50*, 2532.
41. (a) Guilloreau, L.; Damian, L.; Coppel, Y.; Mazarguil, H.; Winterhalter, M.; Faller, P. *J. Biol. Inorg. Chem.* **2006**, *11*, 1024. (b) Atwood, C. S.; Scarpa, R. C.; Huang, X.; Moir, R. D.; Jones, W. D.; Fairlie, D. P.; Tanzi, R. E.; Bush, A. I. *J. Neurochem.* **2000**, *75*, 1219.
42. (a) Mold, M.; Ouro-Gnao, L.; Wieckowski, B. M.; Exley, C. *Sci. Rep.* **2013**, *3*. (b) Sharma, A. K.; Pavlova, S. T.; Kim, J.; Finkelstein, D.; Hawco, N. J.; Rath, N. P.; Kim, J.; Mirica, L. M. *J. Am. Chem. Soc.* **2012**, *134*, 6625.
43. Faller, P.; Hureau, C.; Berthoumieu, O. *Inorg. Chem.* **2013**, *52*, 12193.
44. Liu, Y.; Kochi, A.; Pithadia, A. S.; Lee, S.; Nam, Y.; Beck, M. W.; He, X.; Lee, D.; Lim, M. H. *Inorg. Chem.* **2013**, *52*, 8121.